

A pharmacodynamic model of Aurora kinase inhibitors in the spindle assembly checkpoint

Hitesh B. Mistry¹, David E. MacCallum², Robert C. Jackson², Mark A. J. Chaplain¹, Fordyce A. Davidson¹

¹Division of Mathematics, University of Dundee, Dundee DD1 4HN, Scotland, UK, ²Cyclacel Ltd., James Lindsay Place, Dundee DD1 5JJ, Scotland, UK

TABLE OF CONTENTS

1. Abstract
2. Introduction
 - 2.1. Aurora kinases and the spindle assembly checkpoint
 - 2.2. Pharmacodynamic modelling
3. Model construction
 - 3.1. Aurora kinase activity and biomarkers
 - 3.2. Kinetochore-microtubule attachment transitions
 - 3.3. Spindle assembly checkpoint
4. Results
 - 4.1. Strict inhibitors
 - 4.1.1. Aurora-A inhibition
 - 4.1.2. Aurora-B inhibition
 - 4.2. Combined inhibitors
 - 4.2.1. Additive inhibition
 - 4.2.2. Mixed inhibition
5. Discussion
6. Acknowledgements
7. References

1. ABSTRACT

Arguably the most dramatic phase in the cell cycle is mitosis, during which replicated chromosomes are sorted into two distinct sets. Aurora kinases are central to the accurate segregation of chromosomes during mitosis. Consequently, they have been selected as possible targets for cancer therapy. Anti-cancer drugs that target Aurora kinases are normally designed to inhibit their function. The complexity of the roles of Aurora kinases and their interaction with respective inhibitors means that it is often very difficult to obtain meaningful links between inhibitor concentration and efficacy using standard methods. To overcome these difficulties, we propose a novel mathematical modelling approach. We present a pharmacodynamic model that is able to encapsulate the key roles of two kinases, Aurora A and B, in the spindle assembly checkpoint. Moreover, the model is capable of qualitatively differentiating between the effects of inhibiting Aurora A, Aurora B and A plus B, respectively, by predicting cell behaviour. Consequently, predictions regarding the qualitative relationship between inhibitors, measurable biomarkers and cell damage can be obtained using this powerful modelling approach.

2. INTRODUCTION

The faithful separation of chromosomes prior to cell division at mitosis is essential for maintaining genomic integrity. Failure to do so correctly may lead to genomic instability, aneuploidy and cancer (1-3). Chromosome segregation requires the formation of a microtubule network that connects the spindle poles, located at either end of the cell, to kinetochores (protein structures located at the centromeres of each chromosome) (4). This is a highly regulated process involving the interactions between multiple protein complexes and signalling pathways (3, 5). One family of serine/threonine kinases that play a central role in regulation is the Aurora family consisting of three forms in metazoans: Aurora A, Aurora B and Aurora C. In fission yeast and budding yeast only one homologue is found (Ark1 and Ipl1 respectively) (6-8). Aurora C is only expressed in germ cells, whereas Aurora A and Aurora B are found in all proliferating cells (6). Significantly, all three Aurora kinases are over-expressed in a variety of cancers, suggesting a growth advantage is gained by their deregulation (5, 9). Furthermore, severe inhibition of Aurora kinase activity leads to a failed mitosis (7, 10-17). Hence, this form of inhibition provides a possible

A pharmacodynamic model of Aurora kinase inhibitors

mechanism for the selective removal of replicating cells and thus has led to the development of Aurora kinase inhibitors as possible anti-cancer drugs (11, 13, 15, 17).

2.1. Aurora kinases and the spindle assembly checkpoint

Aurora B is active throughout mitosis with protein levels peaking at G₂/M phase of the cell cycle (6). It regulates chromosome congression, segregation and cytokinesis (6, 14). Aurora B forms a complex with INCENP and survivin that regulate its activity and localisation throughout mitosis (18-20). Proteins of the Aurora B complex are “chromosome passengers” localised to the centromeres from prophase until the metaphase-anaphase transition at which time Aurora B relocates to the spindle mid-zone and equatorial cell cortex as well as to the microtubules (19). During telophase Aurora B localises to the mid-body (6, 8, 20).

In budding yeast, the Aurora B homologue, Ipl1, can promote correct spindle assembly by destabilising syntelic attachments (21, 22). Its role in destabilising attachments has also been demonstrated in mammalian cells for syntelic attachments (13, 23) and merotelic attachments (24). Aurora B promotes turnover of microtubules at the kinetochores (14) possibly by regulating Hec 1 (25). Aurora B is also required for cytokinesis where it phosphorylates and regulates several substrates (7, 8). Characterisation of Aurora B inhibitors have suggested that it plays a role in the spindle assembly checkpoint, in part by destabilising the localisation of BubR1, Mad2 and Cenp-E at centrosomes (13, 26), and responds to changes in tension to promote biorientation (13, 23, 27, 28). Treatment of cells with Aurora B inhibitors causes chromosome alignment problems, spindle checkpoint override and cytokinesis failure, broadly consistent with data generated by other methods (13, 15, 17).

The level of Aurora A activity increases during G₂ phase and the kinase is phosphorylated and activated at this stage. In G₂ phase and early mitosis, Aurora A localises to centromeres, becoming more abundant on microtubules during metaphase (14). Inhibition of Aurora A by siRNA or small molecules shows that it is required for mitotic commitment, centrosome maturation and separation (7, 10-12, 16). Moreover, depletion of Aurora A in cells that contained a correct bi-polar spindle structure, resulted in a checkpoint dependent prolonged mitosis caused by unstable kinetochore-microtubule attachments (29).

The effects of Aurora kinases on the spindle assembly checkpoint are of particular interest because this checkpoint is crucial to prevent onset of anaphase without proper alignment of chromosomes and correctly attached spindles (30). A wait signal is generated by kinetochores, which inhibits the activation of the anaphase-promoting complex (APC/C). Even one unattached kinetochore is thought to be enough to prevent the onset of anaphase (31). How this process occurs has yet to be fully defined, although a number of models have been proposed (30, 32,

33-36), including mathematical modelling of potential mechanisms (34-36).

2.3. Pharmacodynamic modelling

A key stage in the early testing of drugs in humans is determining the pharmacokinetic (PK) profile i.e. how widely the drug is distributed in the body, how rapidly is it eliminated and what plasma concentrations are attainable. PK modelling has for many years been an established technique in drug development. The predictive power of PK has been maximised by fitting mathematical models, which can be empirical or physiologically based, to data. What PK measurements do not provide, however, is any indication of how effectively the drug is working: this is the province of pharmacodynamics (PD), which studies drug *effects* in the body, rather than drug *concentrations*. In some cases it is possible to infer the PD effect from the plasma concentration: if the dose-response relationship of the drug effect has been established in preclinical test systems, a simple PK-PD model may be constructed by coupling a dose-response equation to a PK model (see e.g. (37, 38)). This works best when the drug effect closely tracks the concentration in the blood (which can be measured) rather than at some other site such as the liver, or the brain, where PK measurements are usually not possible. It also works best when the drug effect closely tracks the drug concentration in time. When these conditions are not met, then the relationship between drug concentration and drug efficacy breaks down and therefore the usefulness of traditional PK models is limited. In these cases PD data and modelling are vital.

One important example of where the relationship between PK and PD data is not in general known is in the action of anti-cancer drugs. For these drugs the effects, *in vivo*, are often not measurable until several weeks after administration, by which time a negative response could render further, alternative therapies redundant. Therefore it is vital to develop a fast and accurate test for drug efficacy. We believe that appropriate PD models will provide core information for any such predictive tool.

In this paper we introduce a new PD modelling framework, which focuses on the action of a class of anti-cancer drugs known as Aurora kinase inhibitors. It utilises the mathematical model introduced in (36), which was the first to provide a mechanistic, mathematical description of the chromosome attachment process and the spindle assembly checkpoint in metazoan cells. The mathematical framework detailed below has been developed in combination with experimental data to make testable predictions regarding the effects of kinase activity inhibition. In particular, it is shown that the model predicts specific and qualitatively distinguishable outcomes resulting from Aurora A, Aurora B and mixed inhibition, respectively. Furthermore, the model yields a PD relationship between inhibitor concentration and measurable biomarker endpoints.

In the construction of any new mathematical modelling framework, tension always arises between the

A pharmacodynamic model of Aurora kinase inhibitors

inclusion of biological detail and mathematical tractability. We believe that it is *not* the goal of the mathematical modeller to form an extremely complex system of equations in an attempt to mirror reality. All that achieves is the replacement of one form of impenetrable complexity with another. Instead, the aim is to reduce a complex (biological) system to a simpler (mathematical) system where the rigorous, logical structure of the latter can be used to identify, isolate and investigate key properties.

3. MODEL CONSTRUCTION

We now describe a PD model for key processes in the spindle assembly checkpoint. As alluded to above, these processes are extremely complex. However, our aim is to develop a minimal model that can be interrogated in a meaningful, qualitative manner, regarding the principal action of Aurora A and B activity and the effects of inhibiting such activity. This requires the construction of a model that describes these functional interactions at an appropriate scale.

3.1. Aurora kinase activity and biomarkers

During inhibition studies, both *in vitro* and *in vivo* concentration levels of active Aurora kinase are normally calculated by analysing the concentration of a kinases-specific biomarker. Biomarkers identified for Aurora A and B are phosphorylated Aurora A and phosphorylated histone H3, respectively. We will make use of these relationships.

To describe the level of Aurora kinase activity in the model set up, we employ the following argument. Let A and B denote the relative activity of Aurora kinase A and B, respectively. Denote the concentration of the corresponding inhibitors $[A^-]$ and $[B^-]$. The activity levels A and B are functions of their respective inhibitor concentrations and we assume that they are normalized so that in the absence of any inhibitor $A(0) = B(0) = 1$. Define the concentration $[A^-] = IC_{50}^A$ where $A(IC_{50}^A) = 0.5$, as is standard, i.e. it is the concentration of inhibitor required to reduce activity by 50%. A definition IC_{50}^B follows similarly.

We now relate the relative activity A defined above to experimentally observed data. Following the present general consensus, we make two central assumptions. First, using similar arguments to those in (37), a relationship between the relative activity, A_p , of biomarker for Aurora A activity (auto-phosphorylation of Aurora A at T288) and the inhibitor of that activity, $[A^-]$, can be defined as

$$A_p = 1 - \frac{[A^-]^n}{(IC_{50}^A)^n + [A^-]^n}, \quad [1]$$

where n and IC_{50}^A are chosen to fit the observed experimental data from biomarker studies. Second, we assume that $A = A_p$ (see e.g. (15, 16, 17) and the references

therein). Hence, a relationship between kinase activity and inhibitor concentration follows directly from [1].

For the relative activity B , we again assume that it is directly related to the relative activity of its biomarker. Thus a relationship between Aurora B activity and its inhibitor concentration can be derived using [1] with the obvious notational changes. (The biomarker for Aurora B activity is phosphorylation of histone H3 at S10.)

3.2. Kinetochores-microtubule attachments

A human cell contains 23 pairs of chromosomes, which are duplicated during mitosis, resulting in 46 pairs of chromosomes, each with 2 kinetochores. Each kinetochore is known to have between 20-30 microtubule binding sites (39). Kinetochore-microtubule attachment is a very complex process involving a cascade of mechano-chemical reactions (31) occurring throughout prometaphase. It is not the aim in this paper to investigate the details of this complex attachment process. Rather, we will simply concern ourselves with the temporal evolution of "attachment type" as we now discuss.

Proper chromosome segregation requires sister kinetochores to form an amphitelic attachment, where sister kinetochores are bound to microtubules from opposite spindle poles. However, three types of incorrect attachment can occur that lead to a mis-segregation of chromosomes: (i) (complete) unattachment; (ii) syntelic attachment (both sister kinetochores are bound to microtubules from the same pole); (iii) merotelic attachment (one sister kinetochore is bound to microtubules from both spindle poles), see Figure 1A. One further type of attachment (monotelic) is common in the very early stages of prometaphase. However, these exist only as brief, transitory states in the subsequent attachment process (40-42). Therefore, we do not consider these further.

Syntelic and merotelic attachments are observed throughout prometaphase, predominantly in the earlier stages (13, 43). The correction process of these attachment types can be summarised as follows. Syntelically attached kinetochores are drawn towards the corresponding spindle pole. Subsequently, the aberrant attachments are released via the action of Aurora B kinase (13, 15) and after relocating to the metaphase plate it is common that these kinetochore pairs form amphitelic attachments (42). Merotelically attached kinetochores are aligned at the spindle equator, where Aurora B destabilises the aberrant attachments, thus allowing the sister kinetochores to almost immediately become amphitelicly attached (40).

A key substrate involved in making proper kinetochore-microtubule attachments is CENP-A and this has been identified as a target of both Aurora A and B kinase: CENP-A is sequentially phosphorylated first by Aurora A in prophase and then by Aurora B (29). However, phosphorylation of CENP-A is not required to make a kinetochore-microtubule attachment (29). Rather, it appears to be essential to stabilise the attachment (29).

A pharmacodynamic model of Aurora kinase inhibitors

Table 1. List of parameter values

Parameter	Value
k_1'	0.178 min^{-1}
k_2'	0.02 min^{-1}
k_3'	0.04 min^{-1}
k_4'	0.3 min^{-1}
k_5'	0.2 min^{-1}
k	$0.004 \text{ } \mu\text{m}^3 \text{ s}^{-1}$
k_k	$30 \text{ } \mu\text{m}^3 \text{ s}^{-1}$
v_c	$6000 \text{ } \mu\text{m}^3$
α	0.2 min^{-1}
α_c	0.2 min^{-1}
α_a	0.2 min^{-1}
A_c	0.5

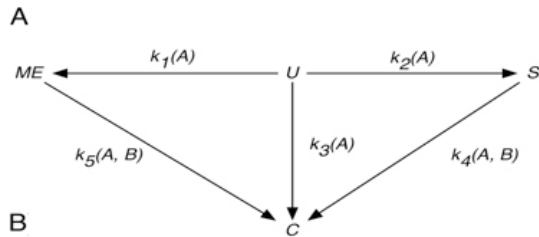
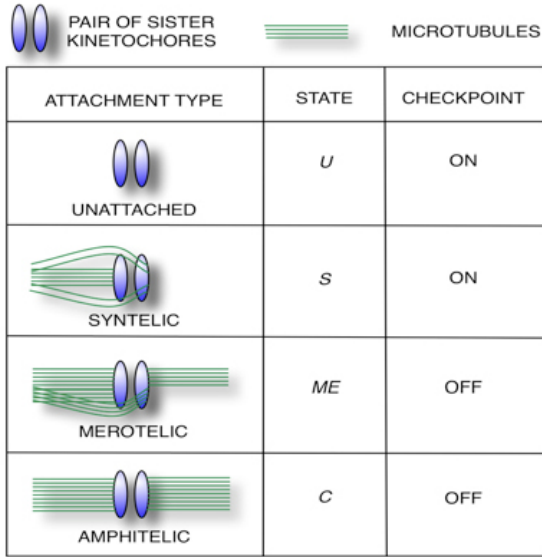


Figure 1. Kinetochores microtubule attachment schematic: (A) table showing the different types of attachments possible, how each type of attachment corresponds to variables within the model framework and their effect on the spindle assembly checkpoint; (B) network diagram showing the possible states each kinetochores unit could be in at any given time and how they can move from state to state. (See text for detailed description)

In the following, we define a pair of sister kinetochores as a *unit*. We assume that both kinetochores within the unit have all their binding sites occupied or both kinetochores have binding sites available (40-42). We assume further that these two sets can be divided as follows: a unit displaying full occupancy can be in either a merotelic (*ME*) or amphitelic (*C*) state; otherwise it is deemed to be in a syntelic (*S*) or unattached (*U*) state (40-42). Following

the above arguments a unit state transition network can be constructed, see Figure 1B. The parameters, $k_i(A)$ ($i=1, \dots, 3$) and $k_j(A, B)$ ($j=4, 5$) in Figure 1B, represent the rates at which a unit undergoes the corresponding state transition within a single cell. We assume that the concentration of Aurora A and B affect the transition rates in the following way. The roles Aurora A and B play in stabilising attachments (29) and releasing aberrant attachments for subsequent repair (13, 23) are respectively modelled by assuming that the rate constants k_i and k_j are positively correlated to the values of *A* and *B*. Furthermore we assume that *A* only affects a fraction, A_C , of k_i and k_j (29). In lieu of further experimental evidence, we assume these relationships to be linear i.e.,

$$\begin{aligned} k_i(A) &= k_i'(1 - (1 - A)A_C) \text{ min}^{-1}, \\ k_j(A, B) &= k_j'(1 - (1 - A)A_C)B \text{ min}^{-1}, \end{aligned} \quad [2]$$

for constants k_i' , k_j' and A_C with $A_C < 1$.

Let $\langle X_i \rangle$ denote the expected mean number of kinetochores units in a state *i* in any given cell within a large population of genetically identical cells. The total number of units is conserved, so that,

$$\langle X_U(0) \rangle = 46 = \langle X_U(t) \rangle + \langle X_S(t) \rangle + \langle X_{ME}(t) \rangle + \langle X_C(t) \rangle.$$

Using this relationship, the temporal evolution of each $\langle X_i \rangle$ is given by the following system of ordinary differential equations (odes),

$$\begin{aligned} \frac{d\langle X_U \rangle}{dt} &= -(k_1(A) + k_2(A) + k_3(A))\langle X_U \rangle, \\ \frac{d\langle X_S \rangle}{dt} &= k_2(A)\langle X_U \rangle - k_4(A, B)\langle X_S \rangle, \\ \frac{d\langle X_{ME} \rangle}{dt} &= k_1(A)\langle X_U \rangle - k_5(A, B)\langle X_{ME} \rangle. \end{aligned} \quad [3]$$

We define, $D(t) = \langle X_U(t) \rangle + \langle X_S(t) \rangle + \langle X_{ME}(t) \rangle$ to be the expected mean number of aberrant units at any given time, *t*. For a detailed derivation of the above system we direct the reader to (36). Parameter values are given in Table 1 and a summary of the system variables is given in Table 2.

3.3. Spindle assembly checkpoint

The spindle assembly checkpoint model constructed by Mistry *et al.* (36), concerns the wait signal generated by the *temporal evolution* of kinetochores-microtubule attachments. For a detailed description of the model and related background, we direct the reader to (34, 36). Here, we present a brief summary. From the above discussions it is reasonable to assume that a wait signal is generated from each *U* and *S*-type unit, the reaction processes being given by,

A pharmacodynamic model of Aurora kinase inhibitors

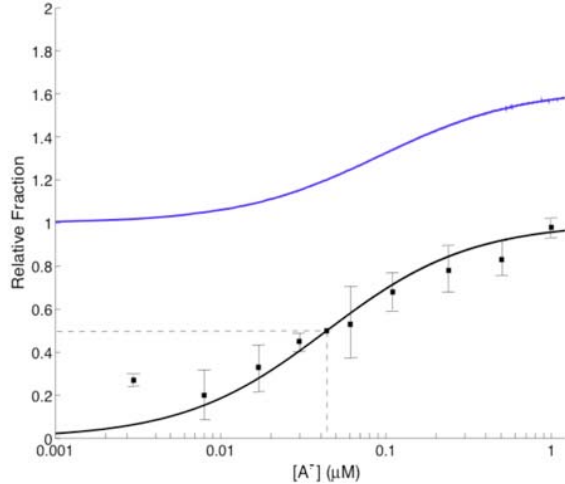
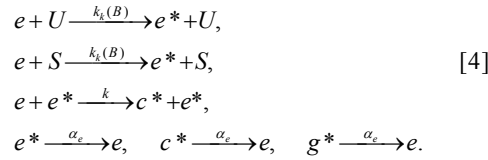


Figure 2. Plot showing t_a/t^* where $t^* = t_a(A=1=B)$ (blue line) and $1-A$ (black line) as functions of $[A^-]$. (The black squares denote experimental data points from (44)).



Here, species e is associated with free Cdc20, a known activator of the APC/C. We assume that units in either the U or S state can generate inhibited complexes of Cdc20, denoted by e^* , at a diffusion limited rate, $k_k = B k_k'$, where $k_k' = 30 \mu\text{m}^3 \text{s}^{-1}$ (36). Note, to the authors' best knowledge, the production rate of e^* is state independent. It is assumed that the inhibited complex e^* can catalyze the production of further inhibited complexes of e denoted by c^* , at a diffusion limited protein-protein interaction rate, $k = 0.004 \mu\text{m}^3 \text{s}^{-1}$ (36). As in (34) it is assumed that these complexes, c^* , cannot catalyse further complex formation. We use $\alpha^{-1} = \alpha_e^{-1} = 5 \text{ min}$ (34). Species g^* is associated with inhibitory complexes of Cdc20 generated prior to prometaphase and by a different mechanism (36). This complex decays releasing the Cdc20 at a rate, $\alpha_g^{-1} = 5 \text{ min}$ (36).

Finally, define N_x to be the total number of molecules of species $x \in \{e, e^*, c^*, g^*\}$. The total number of molecules is conserved, so that, $N = N_e + N_{e^*} + N_{c^*} + N_{g^*}$ ($N = 800000$ (34)). Using this relationship, we model the dynamics of the spindle assembly checkpoint as system [3] combined with the following system of odes,

$$\begin{aligned}
 \frac{dN_{e^*}}{dt} &= -\frac{k_k(B)}{v_c} (\langle X_U \rangle + \langle X_S \rangle) N_e - \alpha_e N_{e^*}, \\
 \frac{dN_{c^*}}{dt} &= -\frac{k}{v_c} N_e N_{e^*} - \alpha_c N_{c^*}, \\
 \frac{dN_{g^*}}{dt} &= -\alpha_g N_{g^*},
 \end{aligned} \tag{5}$$

where, $v_c = 6000 \mu\text{m}^3$ is the cytoplasmic volume (34).

Recall each unit of type i comprises two kinetochores with the expected value $\langle X_i \rangle \in [0, 46]$. However, if $\langle X_i \rangle < 0.5$, then this expected value corresponds, in some sense, to the presence of less than a single kinetochore. Therefore in system [5] we assume that, if $\langle X_i \rangle < 0.5$, then $\langle X_i \rangle \equiv 0$. This leads to the definition,

$$t_f = \min \{t \geq 0 \mid \langle X_S(t) \rangle \leq 0.5 \ \& \ \langle X_U(t) \rangle \leq 0.5\},$$

which best represents the time at which the last kinetochore is sensed by system [5]. Furthermore, following (34), we define the time to anaphase (length of prometaphase/metaphase) as

$$t_a = \max \{t \geq 0 \mid N_e \leq 200000\}.$$

4. RESULTS

4.1. Strict Inhibitors

We first consider the action of strict Aurora kinase inhibitors. These are inhibitors that are assumed to inhibit the function of either Aurora A or B only.

4.1.1. Aurora-A inhibition

Throughout this subsection, we assume there is no Aurora B inhibition, that is $B = 1$.

Manfredi *et al.* (44) investigated certain properties of an Aurora kinase inhibitor (MLN8054), which is reported to be a potent and selective inhibitor of Aurora A. In their study, amongst other results, they determined the IC_{50}^A value for Aurora A activity in HeLa cells. In what follows, we use this value ($IC_{50}^A = 0.044 \mu\text{M}$) and to provide a best fit to the experimental dataset in (44), we set $n = 1$ in [1], see Figure 2.

It is known that Aurora A inhibition can result in acentrosomal spindle poles (16). Clearly, for very low values of inhibition, it is likely that most cells will retain correct bi-polar spindles. However, in (16) it was shown that $0.25 \mu\text{M}$ of MLN8054 resulted in at most 30% of cells displaying correct bi-polarity. Of course, this does not rule out that any given cell may retain correct bi-polarity even at high concentrations of inhibitor. As a first step, we assume in the model that all cells retain correct bi-polar spindles for the range of values of the inhibitor considered. We note that most of the behaviour shown in Figure 2 corresponds to concentrations of the inhibitor less than $0.25 \mu\text{M}$.

By systematically increasing the value of $[A^-]$ from zero, it was observed that the time to anaphase, t_a , remained essentially unchanged over a significant range of values, see Figure 2. For low values this provides evidence that the model is not overly sensitive to small changes in

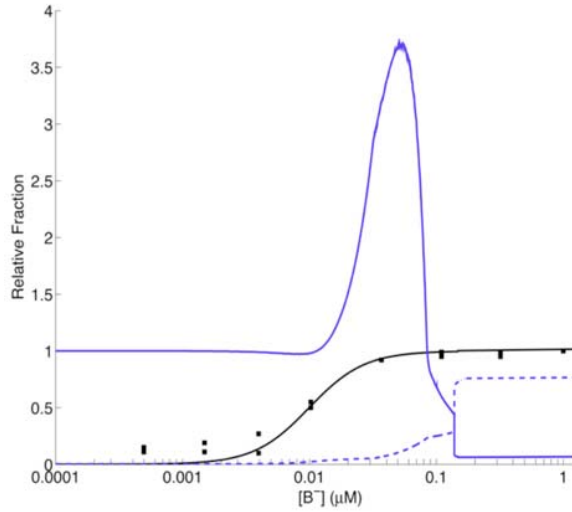


Figure 3. Plot showing t_a/t^* (blue solid line), $D(t_a)/D(0)$ (blue dashed line) and $1-B$ (black line) as functions of $[B^-]$. (The black squares denote experimental data points from (17)).

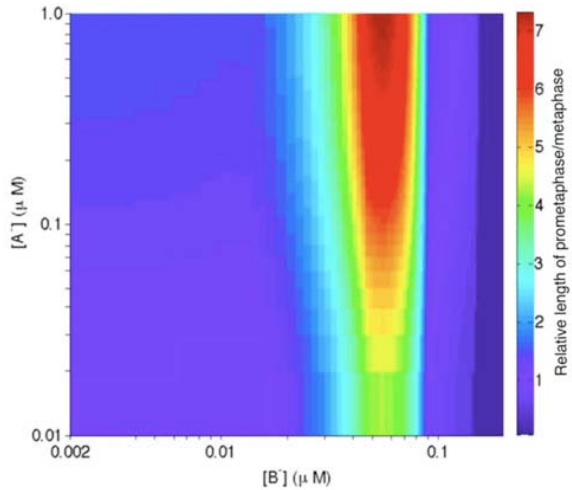


Figure 4. Plot showing the relative length of prometaphase/metaphase, t_a/t^* , as a function of both $[A^-]$ and $[B^-]$.

the values of the parameters k_i' ($i=1,\dots,5$) chosen to represent the uninhibited state. On increasing $[A^-]$ further, t_a exhibits a smooth increase before appearing to level out at a limiting value. This can be explained as follows. Increasing $[A^-]$ leads to a reduction in all rates k_i ($i=1,\dots,5$) in [2]. Consequently units linger in the U , S and ME state. The U and S type units are detected by the correctly functioning spindle checkpoint mechanism [5]. Therefore an increase in t_a is observed due to an increase in t_f . The appearance of a limiting value for t_a , as $[A^-]$ increases, is a direct result of the functional form of the rates $k_i(A)$ given in [2].

4.1.2. Aurora-B inhibition

Throughout this subsection, we assume there is no Aurora A inhibition, that is $A = 1$.

Wilkinson *et al.* (17) reported on experiments concerning a known potent and selective Aurora B inhibitor, AZD1152. They determined the IC_{50}^B value in SW620 cells. In what follows we use this value ($IC_{50}^B = 0.01027 \mu M$) and to provide the best fit to the experimental dataset in (17), we set $n=2$ in [1], see Figure 3.

The qualitative results regarding Aurora B inhibition are discussed in detail in (36). Here we present a brief overview of the effects of Aurora B inhibition on systems [3] and [5]. From Figure 3 it can be seen that on systematically

increasing the value of $[B^-]$, both t_a and $D(t_a)$ remain almost unchanged for low to mid-range levels of inhibition. (This provides further evidence of the robustness to parameter values

mentioned above.) On increasing $[B^-]$ further, a rapid increase in t_a is observed, but $D(t_a)$ still does not change significantly. The increase in t_a is a consequence of a reduction in the rate k_d , which leads to lingering S type units that are detected by the correctly functioning spindle checkpoint mechanism [5]. Therefore an increase in t_a is observed due to an increase in t_f .

A notable change in t_a and $D(t_a)$ is evident when $[B^-] \approx 0.03$

μM , at which point, $t_a = t_f$. Increasing $[B^-]$ beyond this value gives $t_a < t_f$, resulting, by definition, in a significant increase in $D(t_a)$. Thereafter, t_a reaches a peak value before dropping sharply as a consequence of the weakening of the wait signal generated by [5]. Finally, at high levels of inhibition a catastrophe in the system dynamics occurs at which point, the values t_a and $D(t_a)$ jump discontinuously to values that remain unaltered by further increasing $[B^-]$. This occurs due to the release of e from the decay of g^* dominating the system dynamics, resulting in an almost immediate onset of anaphase, with corresponding high levels of incorrectly attached units.

4.2. Combined inhibitors

The simultaneous inhibition of Aurora A and B can be achieved either by simply combining (strict) Aurora A and B inhibitors or through a single, mixed inhibitor. We now explore each of these possibilities in turn.

4.2.1. Additive inhibition

For ease of comparison with the action of strict inhibitors, we again use $IC_{50}^A = 0.044 \mu M$ and $IC_{50}^B = 0.01027 \mu M$.

From the above results on the action of strict Aurora A and B inhibitors, it is straight forward to ascertain the effects of purely additive inhibition (that is a combination of inhibitors that do not interact). For fixed $[B^-]$, an increase in $[A^-]$ results in an increase in t_a . Moreover, the range of $[B^-]$ values for which an increase in t_a is observed, becomes broader for increasing $[A^-]$. These results are summarised in Figure 4. Finally,

A pharmacodynamic model of Aurora kinase inhibitors

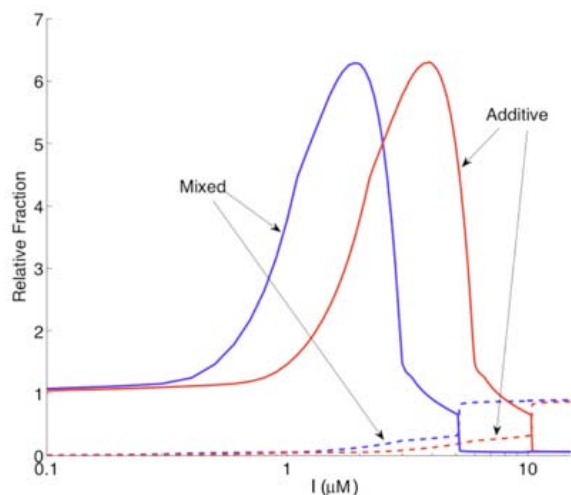


Figure 5. Plot showing the relative time to anaphase t_a/t^* (solid lines) and predicted number of aberrant attachment units (dashed lines) as functions of $[Z]$. Blue lines represent the mixed inhibitor. Red lines represent the additive inhibitor with $[Z]=[A^-]+[B^-]$. In both cases $IC_{50}^{A_z} = IC_{50}^{B_z} = 0.35\mu M$

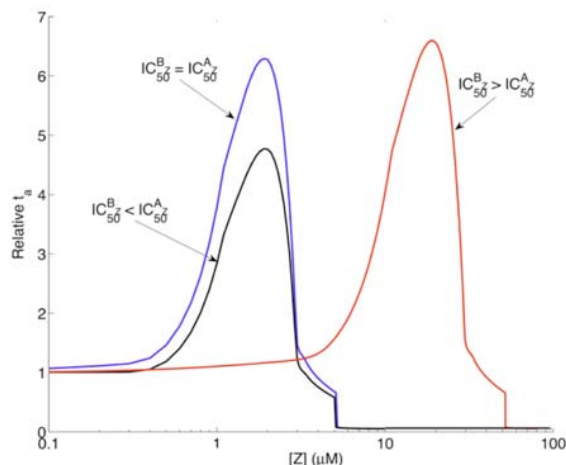


Figure 6. Plot showing the relative time to anaphase, t_a/t^* , as a function of $[Z]$ for different IC_{50} values: black line $IC_{50}^{B_z} < IC_{50}^{A_z}$; blue line $IC_{50}^{B_z} = IC_{50}^{A_z}$; red line $IC_{50}^{B_z} > IC_{50}^{A_z}$. For IC_{50} values see text.

systematically increasing $[A^-]$ has little or no effect on the fraction of aberrant attachments for any value of $[B^-]$ (data not shown).

We repeated the above procedure using $IC_{50}^A = IC_{50}^B = 0.35\mu M$, see Figure 5. This allows for a direct comparison with mixed inhibition discussed in the next section.

4.2.2. Mixed inhibition

We now consider a single, mixed inhibitory agent, denoted by Z , which is assumed to interact with both

Aurora A and B molecules. An example of such a compound is ZM44743 (45). *In vivo* data regarding the activity of this dual Aurora kinase inhibitor was investigated for Calu6 cells in (45), where it was shown that $IC_{50}^{B_z} < IC_{50}^{A_z}$. From Figure 1A in (45) it can be read off that $IC_{50}^{B_z} = 0.35\mu M$ & $IC_{50}^{A_z} = 2.19\mu M$. (Note that the first value is different to that quoted in Figure 1A in (45)). To incorporate mixed inhibition into the model we replace [1] with,

$$A = 1 - \frac{[Z]^{n_A}}{(IC_{50}^{A_z})^{n_A} + [Z]^{n_A}}, \quad [6]$$

$$B = 1 - \frac{[Z]^{n_B}}{(IC_{50}^{B_z})^{n_B} + [Z]^{n_B}}, \quad [7]$$

and use these expressions in [2], which are subsequently used in [3] and [5]. Here, $n_A = 1$ and $n_B = 2$ were chosen to fit the experimental data in (45) (not shown here).

First, we assume that the IC_{50} values are those found in (45) and given above. By systematically increasing the value of $[Z]$, we observe that in this case, the qualitative effects of mixed inhibition are similar to that of strict Aurora B inhibition, cf. Figures 3 and 6. This is a direct consequence of the chosen IC_{50} values and their respective effects on the response functions given in [6] and [7].

We now wish to use the model to directly compare additive with mixed inhibition. To this end we now suppose that Z has an equal affinity for both Aurora A and B (i.e. $IC_{50}^{A_z} = IC_{50}^{B_z} = 0.35\mu M$). It can be seen from Figure 5 that for small total values of inhibitor the resultant effect on t_a of additive or mixed inhibition is very similar. However, on increasing the total concentration of the inhibitory agent, the mixed inhibitor appears to act synergistically. The maximum of t_a occurs at a lower concentration of mixed inhibitor than that for an additive inhibitor (cf. the solid lines in Figure 5). Moreover, the discontinuous jump in t_a is achieved using approximately 50 percent less mixed inhibitor than total additive inhibitor. Finally, it follows from the model that more aberrant attachments are induced by the mixed inhibitor than the additive inhibitor at any fixed inhibitor concentration (see dashed lines in Figure 5).

For completeness, we reconsider a single mixed inhibitor and compare the effects of varying the respective IC_{50} values. By fixing $IC_{50}^{B_z}$ and on comparing different potencies for Aurora A (i.e. changing $IC_{50}^{A_z}$), the model predicts that on increasing the potency, the maximum value of t_a occurs at approximately the same concentration of $[Z]$ but this maximum value is significantly increased. Moreover, the t_a values are generally higher across the range of $[Z]$, cf. blue and black lines in Figure 6. Now supposing $IC_{50}^{A_z}$ to be fixed and changing the inhibitor's potency for Aurora B (i.e. changing $IC_{50}^{B_z}$), it is observed that on increasing the potency, the position of the

A pharmacodynamic model of Aurora kinase inhibitors

Table 2. List of main model variables with descriptions (all are functions of time t)

Variable	Description
A	Relative activity of Aurora kinase A
B	Relative activity of Aurora kinase B
$[A]$	Concentration of Aurora A inhibitor
$[B]$	Concentration of Aurora B inhibitor
$[Z]$	Concentration of mixed/ additive inhibitor
X_U	Number U type units
X_S	Number S type units
X_{ME}	Number ME type units
X_C	Number C type units
D	Total number of aberrant units
N_e	Number of free Cdc20 molecules
N_e^*	Number of C-Mad2-Cdc20/BubR1-Cdc20 complex
N_c^*	Number of C-Mad2-Cdc20/BubR1-Cdc20 complex
N_g^*	Number of inhibitory complexes of Cdc20 created in prophase

maximum of t_a occurs at a much lower value of $[Z]$ but this maximum value is significantly reduced, cf. red and black lines in Figure 6.

The above results are not intuitive but arise from a straightforward consideration of the rate constants in the model. The dual role of $[Z]$ in both [6] and [7] induces a greater effect on the rate constants in [3] and [5] than the individual roles of the strict inhibitors detailed in [1] and the corresponding equation for B . That is the mixed inhibitor provides a greater *effective* concentration than the additive inhibitor at the same dosing level. Changing the potency for Aurora A within a mixed inhibitor effects only the rate constants in system [3]. Consequently, the checkpoint [5] remains effective while the unit state transitions are delayed. Changing the potency for Aurora B within a mixed inhibitor affects the rate constants in both systems [3] and [5]. Consequently, the unit transitions are delayed and now the checkpoint is also compromised.

5. DISCUSSION

In this paper we have introduced a pharmacodynamic model for key processes in the spindle assembly checkpoint mediated by Aurora A and B kinases. The model: (i) is able to differentiate between the inhibition of Aurora A and B by predicting time to anaphase and the resultant number of aberrant kinetochore-microtubule attachments; (ii) predicts that combining Aurora A and B inhibitors can have a positive, effect on efficacy and; (iii) allows for a direct comparison of additive and mixed inhibitors and predicts that mixed inhibitors are more potent than additive inhibitors at a similar dosage. This final point is of particular interest as the model predicts that combining inhibitors into a single, mixed (non-specific) inhibitory agent has a marked synergistic effect: the *effective* concentration of such a mixed inhibitor is considerably higher than that of a comparable combination dose. The model predicts that this is not a small effect, indeed it predicts that catastrophic levels of miss-segregation can be induced by a mixed inhibitor at approximately half the dose required for a combination treatment to induce the same effect.

Predictions regarding the qualitative relationship between the concentration of measurable biomarkers and cell damage (aberrant attachments) and time to anaphase onset can be derived from the model. These relationships rely on the central hypotheses that: (i) relative biomarker activity can be related to the concentration of its inhibitor by using the formula given in [1] and (ii) that the relative concentration of biomarker for kinase activity is directly related to inhibitor concentration. These appear to the common assumptions in the present literature. The output from the model described here suggests that experimental evidence supporting these assumptions could be found by titrating the inhibitor and recording the corresponding time to anaphase and/or counting aberrant attachments at anaphase onset. These quantities could then be compared with biomarker activity. For example, by plotting time to anaphase as a function of the difference between the control and mediated biomarker concentration, results that are qualitatively similar to those shown in Figures 2–6 should be obtainable if the central assumptions hold.

Another unexpected prediction of the model is that an almost discontinuous jump in the time to anaphase occurs at a critical level of $[B]$. A severely premature onset of anaphase has been observed experimentally (13) for high values inhibition, but this step behaviour has yet to be experimentally verified and represents another testable outcome of the model.

The intention of this work was to construct a tractable mathematical model, which afforded a qualitative analysis of certain key processes. As stated in the introduction, the action of Aurora kinases is extremely complex. Clearly, there are many additions and improvements that could be made to the model proposed here, from a more detailed description of the attachment process to a better representation of the role of the Aurora kinases. However, these possible improvements come at some cost, not least because of the lack of experimental evidence that could afford an accurate parameterisation of more complex models. Notwithstanding this, an obvious but difficult first step would be to reconsider the formation of acentrosomal spindle poles as a result of Aurora A inhibition.

Developing mechanistic models of the type proposed here may provide a step towards a better understanding of the action of Aurora kinase inhibitors. The strength of these models is their ability to (theoretically) link drug concentration to measures of efficacy. Experimentally verified models could lead to improved dosing and scheduling in clinical trials and ultimately models may form part of new clinical tools for patient-specific drug treatment.

6. ACKNOWLEDGEMENTS

This work was funded by the EPSRC grant EP/D04859 under the Mathematics for Business Scheme.

7. REFERENCES

1. Kops, G. J., B. A. Weaver & D. W. Cleveland: On the road to cancer: aneuploidy and the mitotic checkpoint. *Nat Rev Cancer*, 5, 773-85 (2005)

A pharmacodynamic model of Aurora kinase inhibitors

2. Weaver, B. A. & D. W. Cleveland: Decoding the links between mitosis, cancer, and chemotherapy: The mitotic checkpoint, adaptation, and cell death. *Cancer Cell*, 8, 7-12 (2005)
3. Li, J. J. & S. A. Li: Mitotic kinases: the key to duplication, segregation, and cytokinesis errors, chromosomal instability, and oncogenesis. *Pharmacol Ther*, 111, 974-84 (2006)
4. O'Connell, C. B. & A. L. Khodjakov: Cooperative mechanisms of mitotic spindle formation. *J Cell Sci*, 120, 1717-22 (2007)
5. Perez de Castro, I., G. de Carcer & M. Malumbres: A census of mitotic cancer genes: new insights into tumor cell biology and cancer therapy. *Carcinogenesis*, 28, 899-912 (2007)
6. Carmena, M. & W. C. Earnshaw: The cellular geography of aurora kinases. *Nat Rev Mol Cell Biol*, 4, 842-54 (2003)
7. Meraldi, P., R. Honda & E. A. Nigg: Aurora kinases link chromosome segregation and cell division to cancer susceptibility. *Curr Opin Genet Dev*, 14, 29-36 (2004)
8. Andrews, P. D.: Aurora kinases: shining lights on the therapeutic horizon? *Oncogene*, 24, 5005-15 (2005)
9. Giet, R., C. Petretti & C. Prigent: Aurora kinases, aneuploidy and cancer, a coincidence or a real link? *Trends Cell Biol*, 15, 241-50 (2005)
10. Marumoto, T., T. Hirota, T. Morisaki, N. Kunitoku, D. Zhang, Y. Ichikawa, T. Sasayama, S. Kuninaka, T. Mimori, N. Tamaki, M. Kimura, Y. Okano & H. Saya: Roles of Aurora-A kinase in mitotic entry and G2 checkpoint in mammalian cells. *Genes Cells*, 7, 1173-82 (2002)
11. Hirota, T., N. Kunitoku, T. Sasayama, T. Marumoto, D. Zhang, M. Nitta, K. Hatakeyama & H. Saya: Aurora-A and an interacting activator, the LIM protein Ajuba, are required for mitotic commitment in human cells. *Cell*, 114, 585-98 (2003)
12. Marumoto, T., S. Honda, T. Hara, M. Nitta, T. Hirota, E. Kohmura & H. Saya: Aurora-A kinase maintains the fidelity of early and late mitotic events in HeLa cells. *J Biol Chem*, 278, 51786-95 (2003)
13. Hauf, S., R. W. Cole, S. LaTerra, C. Zimmer, G. Schnapp, R. Walter, A. Heckel, J. van Meel, C. L. Rieder & J. M. Peters: The small molecule Hesperadin reveals a role for Aurora B in correcting kinetochore-microtubule attachment and in maintaining the spindle assembly checkpoint. *J Cell Biol*, 161, 281-94 (2003)
14. Cimini, D., X. Wan, C. B. Hirel & E. D. Salmon: Aurora kinase promotes turnover of kinetochore microtubules to reduce chromosome segregation errors. *Curr Biol*, 16, 1711-8 (2006)
15. Girdler, F., K. E. Gascoigne, P. A. Eyers, S. Hartmuth, C. Crafter, K. M. Foote, N. J. Keen & S. S. Taylor: Validating Aurora B as an anti-cancer drug target. *J Cell Sci*, 119, 3664-75 (2006)
16. Hoar, K., A. Chakravarty, C. Rabino, D. Wysong, D. Bowman, N. Roy & J. A. Ecsedy: MLN8054, a small-molecule inhibitor of Aurora A, causes spindle pole and chromosome congression defects leading to aneuploidy. *Mol Cell Biol*, 27, 4513-25 (2007)
17. Wilkinson, R. W., R. Oedra, S. P. Heaton, S. R. Wedge, N. J. Keen, C. Crafter, J. R. Foster, M. C. Brady, A. Bigley, E. Brown, K. F. Byth, N. C. Barrass, K. E. Mundt, K. M. Foote, N. M. Heron, F. H. Jung, A. A. Mortlock, F. T. Boyle & S. Green: AZD1152, a selective inhibitor of Aurora B kinase, inhibits human tumor xenograft growth by inducing apoptosis. *Clin Cancer Res*, 13, 3682-8 (2007)
18. Mackay, A. M., A. M. Ainsztein, D. M. Eckley & W. C. Earnshaw: A dominant mutant of inner centromere protein (INCENP), a chromosomal protein, disrupts prometaphase congression and cytokinesis. *J Cell Biol*, 140, 991-1002 (1998)
19. Adams, R. R., S. P. Wheatley, A. M. Gouldsworthy, S. E. Kandels-Lewis, M. Carmena, C. Smythe, D. L. Gerloff & W. C. Earnshaw: INCENP binds the Aurora-related kinase AIRK2 and is required to target it to chromosomes, the central spindle and cleavage furrow. *Curr Biol*, 10, 1075-8 (2000)
20. Honda, R., R. Korner & E. A. Nigg: Exploring the functional interactions between Aurora B, INCENP, and survivin in mitosis. *Mol Biol Cell*, 14, 3325-41 (2003)
21. Tanaka, T. U., N. Rachidi, C. Janke, G. Pereira, M. Galova, E. Schiebel, M. J. Stark & K. Nasmyth: Evidence that the Ipl1-Sli15 (Aurora kinase-INCENP) complex promotes chromosome bi-orientation by altering kinetochore-spindle pole connections. *Cell*, 108, 317-29 (2002)
22. Pinsky, B. A., C. Kung, K. M. Shokat & S. Biggins: The Ipl1-Aurora protein kinase activates the spindle checkpoint by creating unattached kinetochores. *Nat Cell Biol*, 8, 78-83 (2006)
23. Lampson, M. A., K. Renduchitala, A. Khodjakov & T. M. Kapoor: Correcting improper chromosome-spindle attachments during cell division. *Nat Cell Biol*, 6, 232-7 (2004)
24. Knowlton, A. L., W. Lan & P. T. Stukenberg: Aurora B is enriched at merotelic attachment sites, where it regulates MCAK. *Curr Biol*, 16, 1705-10 (2006)
25. DeLuca, J. G., W. E. Gall, C. Ciferri, D. Cimini, A. Musacchio & E. D. Salmon: Kinetochore microtubule dynamics and attachment stability are regulated by Hec1. *Cell*, 127, 969-82 (2006)

A pharmacodynamic model of Aurora kinase inhibitors

26. Ditchfield, C., V. L. Johnson, A. Tighe, R. Ellston, C. Haworth, T. Johnson, A. Mortlock, N. Keen & S. S. Taylor: Aurora B couples chromosome alignment with anaphase by targeting BubR1, Mad2, and Cenp-E to kinetochores. *J Cell Biol*, 161, 267-80 (2003)
27. Dewar, H., K. Tanaka, K. Nasmyth & T. U. Tanaka: Tension between two kinetochores suffices for their bi-orientation on the mitotic spindle. *Nature*, 428, 93-7 (2004)
28. Lan, W., X. Zhang, S. L. Kline-Smith, S. E. Rosasco, G. A. Barrett-Wilt, J. Shabanowitz, D. F. Hunt, C. E. Walczak & P. T. Stukenberg: Aurora B phosphorylates centromeric MCAK and regulates its localization and microtubule depolymerization activity. *Curr Biol*, 14, 273-86 (2004)
29. Kunitoku, N., T. Sasayama, T. Marumoto, D. Zhang, S. Honda, O. Kobayashi, K. Hatakeyama, Y. Ushio, H. Saya & T. Hirota: CENP-A phosphorylation by Aurora-A in prophase is required for enrichment of Aurora B at inner centromeres and for kinetochore function. *Dev Cell*, 5, 853-864 (2003)
30. Musacchio, A. & E. D. Salmon: The spindle-assembly checkpoint in space and time. *Nat Rev Mol Cell Biol*, 8, 379-93 (2007)
31. Rieder, C. L., R. W. Cole, A. Khodjakov & G. Sluder: The checkpoint delaying anaphase in response to chromosome monoorientation is mediated by an inhibitory signal produced by unattached kinetochores. *J Cell Biol*, 130, 941-8 (1995)
32. Pinsky, B. A. & S. Biggins: The spindle checkpoint: tension versus attachment. *Trends Cell Biol*, 15, 486-93 (2005)
33. Yu, H.: Structural activation of Mad2 in the mitotic spindle checkpoint: the two-state Mad2 model versus the Mad2 template model. *J Cell Biol*, 173, 153-7 (2006)
34. Doncic, A., E. Ben-Jacob & N. Barkai: Evaluating putative mechanisms of the mitotic spindle checkpoint. *Proc Natl Acad Sci U S A*, 102, 6332-7 (2005)
35. Sear, R. P. & M. Howard: Modeling dual pathways for the metazoan spindle assembly checkpoint. *Proc Natl Acad Sci U S A*, 103, 16758-63 (2006)
36. Mistry, H. B., D. E. MacCallum, R. C. Jackson, M. A. J. Chaplain & F. A. Davidson: Modelling the temporal evolution of the spindle assembly checkpoint and role of Aurora B kinase. *Proc Natl Acad Sci U S A*, 105, 20215-20220 (2008)
37. Gabrielsson, J. & D. Weiner: Pharmacokinetic and Pharmacodynamic Data Analysis: Concepts and Applications. Swedish Pharmaceutical Press, (2000)
38. Jackson, R. C.: Predictive software for drug design and development. *Pharm. Dev. Reg.*, 1, 159-168 (2003)
39. McEwen, B. F., A. B. Heagle, G. O. Cassels, K. F. Buttle & C. L. Rieder: Kinetochore fiber maturation in PtK1 cells and its implications for the mechanisms of chromosome congression and anaphase onset. *J Cell Biol*, 137, 1567-80 (1997)
40. Cimini, D.: Detection and correction of merotelic kinetochore orientation by Aurora B and its partners. *Cell Cycle*, 6, 1558-64 (2007)
41. Rieder, C. L. & E. D. Salmon: The vertebrate cell kinetochore and its roles during mitosis. *Trends Cell Biol*, 8, 310-8 (1998)
42. Kapoor, T. M., M. A. Lampson, P. Hergert, L. Cameron, D. Cimini, E. D. Salmon, B. F. McEwen & A. Khodjakov: Chromosomes can congress to the metaphase plate before biorientation. *Science*, 311, 388-91 (2006)
43. Cimini, D., B. Moree, J. C. Canman & E. D. Salmon: Merotelic kinetochore orientation occurs frequently during early mitosis in mammalian tissue cells and error correction is achieved by two different mechanisms. *J Cell Sci*, 116, 4213-25 (2003)
44. Manfredi, M. G., J. A. Ecsedy, K. A. Meetze, S. K. Balani, O. Burenkova, W. Chen, K. M. Galvin, K. M. Hoar, J. J. Huck, P. J. LeRoy, E. T. Ray, T. B. Sells, B. Stringer, S. G. Stroud, T. J. Vos, G. S. Weatherhead, D. R. Wysong, M. Zhang, J. B. Bolen & C. F. Claiborne: Antitumor activity of MLN8054, an orally active small-molecule inhibitor of Aurora A kinase. *Proc Natl Acad Sci U S A*, 104, 4106-11 (2007)
45. Yang, H., T. Burke, J. Dempsey, B. Diaz, E. Collins, J. Toth, R. Beckmann & X. Ye: Mitotic requirement for Aurora A kinase is bypassed in the absence of Aurora B kinase. *FEBS*, 274, 3385-3391 (2005)

Key Words Mathematical Modelling, Spindle Assembly Checkpoint, Aurora Kinase Inhibitors, Pharmacodynamics, Synergy

Send correspondence to Fordyce A. Davidson, Division of Mathematics, University of Dundee, Dundee, DD1 4HN, Scotland, U.K., Tel: 44-0-1382 384692, Fax: 44-0-1382 385516, E-mail: fdavidso@maths.dundee.ac.uk

<http://www.bioscience.org/current/vol15.htm>